

# ISR physics at *BABAR*

S.Serednyakov\*,

*Budker Institute of Nuclear Physics, Novosibirsk, Russia*

## Abstract

A method of measuring  $e^+e^-$  annihilation cross sections at low energy  $\sqrt{s} < 5$  GeV, using initial-state radiation, is described. Experimental data from the PEP-II B-factory at 10.6 GeV center-of-mass energy, obtained via ISR, are presented. The cross sections are measured for many processes  $e^+e^- \rightarrow 3\pi, 4\pi, 2K\pi, 2K2\pi, 4K, p\bar{p}, \Lambda\bar{\Lambda}, D\bar{D}, \dots$ . From the measured cross sections the parameters of known resonances are improved, the baryons form factors are derived and compared with theory predictions. New states, e.g; Y(4260) and Y(2175), for which the internal structure is not yet established, are observed.

**Physics of the ISR method.** Processes of  $e^+e^-$  annihilation

$$e^+e^- \rightarrow \text{hadrons}, \quad (1)$$

can be studied in a wide center-of-mass (c.m.) energy range at a high luminosity  $e^+e^-$  machine using initial-state radiation (ISR) [1] in the reaction

$$e^+e^- \rightarrow \text{hadrons} + \gamma, \quad (2)$$

with an energetic recoil photon (ISR photon). The following equation [2] relates cross sections of the processes (1) and (2)

$$\frac{d\sigma_{e^+e^- \rightarrow \text{hadrons} + \gamma}(m)}{dm} = \frac{2m}{s} \cdot W(s, x, \theta_0^*) \cdot \sigma(m), \quad (3)$$

where  $s$  is the squared c.m. total energy and  $E_0 = \sqrt{s}/2$  is the c.m. beam energy,  $m$  is the invariant mass of the final state hadrons,  $x = \frac{E_\gamma^*}{E_0} = 1 - \frac{m^2}{s}$ ,  $E_\gamma^*$  and  $\theta_\gamma^*$  are the ISR photon c.m. energy and minimal c.m. polar angle and  $\sigma(m)$  is the  $e^+e^- \rightarrow \text{hadrons}$  cross section. The radiation function  $W(s, x, \theta_0^*)$  [2]

$$W(s, x, \theta_0^*) = \frac{\alpha}{\pi x} \cdot ((2 - 2x + x^2) \cdot \ln \frac{1 + \cos\theta_0^*}{1 - \cos\theta_0^*} - x^2 \cos\theta_0^*) \quad (4)$$

describes the probability of the ISR photon emission, integrated over the ISR photon polar angle  $\theta_\gamma^*$  in limits  $\theta_\gamma^* > \theta_0^*$ ,  $\alpha$  is the fine structure constant. In case of  $\theta_0^* \rightarrow 0$  the function  $W(s, x)$  is modified as follows  $W(s, x) = \frac{\alpha}{\pi x} \cdot (L - 1)(2 - 2x + x^2)$  with  $L = 2 \ln(\sqrt{s}/m_e)$ , where  $m_e$  is an electron mass.

---

\*e-mail: seredn@inp.nsk.su

In recent years many cross section measurements were performed with the *BABAR* detector [3] at the PEP-II asymmetric-energy storage ring using the ISR approach. One can recall, that at PEP-II the 9-GeV electrons collide with the 3.1-GeV positrons at a c.m. energy of 10.6 GeV (the  $\Upsilon(4S)$  resonance). The measured ISR hadronic mass varied in wide limits from  $\sim 1$  GeV/c<sup>2</sup> up to  $\sim 5$  GeV/c<sup>2</sup>.

Since the polar angle distribution of the ISR photon is peaked near  $\theta_\gamma^* = 0, 180^\circ$ , only a small part  $\sim 15\%$  of ISR photons is detected in the *BABAR* calorimeter. Two modes of ISR measurements are used in *BABAR* : 1 - ISR photon is detected in an event and used as the tag, 2 - ISR photon is emitted close to the beam axis and its detection is not required. In the latter case the recoil mass against the hadronic system is expected to be zero. Most of the ISR measurements in *BABAR* are performed in the mode with detection of the ISR photon. Only a few measurements with hadronic mass  $\simeq 4\text{GeV}/c^2$  used the mode without detection of the ISR photon.

The cross-section of particular  $e^+e^-$  annihilation process is calculated from the measured hadronic mass spectrum using the expression

$$\frac{dN}{dm} = \varepsilon(m) R(m) \sigma(m) \frac{dL}{dm}, \quad (5)$$

where  $dL/dm$  is the so called ISR differential luminosity,  $\varepsilon$  is the detection efficiency, and  $R$  is the radiative correction factor. The ISR luminosity is calculated using the total integrated luminosity  $L_0$  and the probability of the ISR photon emission (Eq. 4):

$$\frac{dL}{dm} = W(s, x, \theta_0^*) \frac{2m}{s} L_0. \quad (6)$$

In the mode with the detection of the ISR photon in the *BABAR* calorimeter we have  $30^\circ < \theta_\gamma^* < 150^\circ$  and  $\theta_0^* = 30^\circ$ . The plot of the ISR luminosity in *BABAR* versus hadronic invariant mass with  $L_0=454 \text{ fb}^{-1}$  is shown in Fig.1. The ISR luminosity, integrated over mass range from 2 to 5 GeV/c<sup>2</sup>, is rather high -  $0.63 \text{ fb}^{-1}$ .

The ISR technique allows to utilize the high luminosity of the  $e^+e^-$  factories (PEP-II, KEKB, KLOE), operating at the fixed energy. It is worth to compare the ISR with the direct  $e^+e^-$  experiments. First of all, the ISR technique allows to study the energy range from  $2m_\pi c^2$  up to  $\sqrt{s}$  in a single experiment. The second ISR advantage is that the detection efficiency in the mode with detected ISR photon is finite at the hadron polar angle  $\theta \simeq 0$  (in the hadron system frame). In the direct  $e^+e^-$  experiment the hadrons produced at the very small angles are not seen at all. The next point is that in ISR the detection efficiency is finite at the very threshold of the particular reaction, while in the conventional  $e^+e^-$  experiment the detection efficiency vanishes at the threshold because of the low momenta of produced particles.

But one should mention that the energy resolution and the energy scale calibration accuracy in ISR are worse than in the direct  $e^+e^-$  set up. Also, in the direct  $e^+e^-$  study of narrow resonances one could concentrate the integrated luminosity in the resonance peak and thus have much higher number of events than in the ISR study.

New ISR measurements of  $e^+e^- \rightarrow \text{hadrons}$  cross sections are important because they are used in the calculation of the Standard model parameters such as the muon anomaly  $a_\mu = \frac{g-2}{2}$  and fine structure constant at Z-mass  $\alpha_{em}(s = M_Z^2)$ . At present, there is the considerable

disagreement  $\sim 3\sigma$  between the  $a_\mu$  measurement and calculation; so new accurate cross section data are needed.

In this review the main *BABAR* ISR results are presented. The results are divided into three parts: production of mesons, production of baryons, and resonance physics.

**Production of mesons** The processes of the  $e^+e^-$  annihilation into light mesons ( $\pi$ ,  $K$ ) give the highest contribution to the total hadronic cross section up to 3 GeV. Many reactions have been studied at *BABAR* using ISR. Figure 2 shows the experimental data on the  $e^+e^- \rightarrow \pi^+\pi^-\pi^0$  reaction [4]. One can see that the *BABAR* data well agree with SND measurement [5] below 1.4 GeV and strongly contradict DM2 results [6] at higher energy. The *BABAR* cross section clearly shows two states  $\omega(1420)$  and  $\omega(1650)$ , which are considered as the radial and orbital excitations of  $\omega(783)$ .

The channels  $e^+e^- \rightarrow \pi^+\pi^-\pi^+\pi^-$ ,  $\pi^+\pi^-\pi^0\pi^0$  give the largest contribution to the hadronic vacuum polarization term of  $a_\mu$  above 1 GeV. *BABAR* data in Figs.3,4 show the considerable improvement of the accuracy above 1.4 GeV [7, 8]. In these reactions the  $\omega\pi^0$ ,  $\pi a_1$ ,  $\rho^+\rho^-$ ,  $\rho^0 f^0$  intermediate states dominate. In the channel  $e^+e^- \rightarrow \pi^+\pi^-\pi^0\pi^0$  a peak above 2 GeV (Fig.4) is seen, which can be manifestation of the hypothetical  $\rho(2150)$  or  $\rho'''$  state.

The cross sections of  $e^+e^- \rightarrow 5\pi$ ,  $6\pi$  processes [9, 10] have been measured by *BABAR* from the threshold up to 4.5 GeV in the final states  $2(\pi^+\pi^-)\pi^0$ ,  $2(\pi^+\pi^-)2\pi^0$ ,  $3(\pi^+\pi^-)$ . The final states have very complex structure. As an example, the  $e^+e^- \rightarrow \omega\pi^+\pi^-$  cross section with the domination of the  $\omega(1650)$  state is shown in Fig.5. In the  $e^+e^- \rightarrow 6\pi$  cross section the structure below 2 GeV is seen (Fig.6), which is assumed to correspond to the state with the parameters  $M=1.88\pm 0.03$  GeV/ $c^2$  and  $\Gamma=0.13\pm 0.03$  GeV/ $c^2$  [10].

The channels with kaons are not less interesting. In the  $e^+e^- \rightarrow K^+K^-\pi^0$  and  $e^+e^- \rightarrow K^\pm K_S \pi^\mp$  reactions [11] the  $\phi(1650)$  isoscalar resonance dominates. The cross section for the  $\phi\eta$  and  $\phi\pi^0$  final states have been measured for the first time. In the  $\phi\eta$  final state the candidate for the  $Y(2175)$  or  $\phi''$  state is possibly seen (Fig.7). The processes  $e^+e^- \rightarrow K^+K^-\pi^+\pi^-$ ,  $K^+K^-\pi^0\pi^0$  [12] show domination of the  $\phi(1650)$  in the total cross section and  $K^*(890)$ ,  $K_1(1270)$ ,  $\eta(1500)$  in intermediate states. The cross section of rare processes with kaons  $e^+e^- \rightarrow K^+K^-\pi^+\pi^-\pi^0$ ,  $K^+K^-\pi^+\pi^-\eta$  [9],  $e^+e^- \rightarrow K^+K^-\pi^+\pi^-\pi^+\pi^-$  [10] and  $e^+e^- \rightarrow K^+K^-K^+K^-$  [12] have been also measured by *BABAR* for the first time. The maximum cross section value for these processes is not higher than 1 nb.

The  $e^+e^-$  annihilation into D-mesons was studied by *BABAR* [13] in the mode with undetected ISR photon. The D-mesons ( $D^\pm$ ,  $D^0$ ,  $\bar{D}^0$ ,  $D^{*\pm}$ ,  $D^{0*}$ ,  $\bar{D}^{0*}$ ) are selected via their main decay modes ( $K\pi$ ,  $K2\pi$ ,  $K3\pi$ ). The main goals of this study are to confirm the high mass charmonium states  $\psi(4040)$ ,  $\psi(4160)$ ,  $\psi(4400)$  and look for the recently observed  $Y(4260)$  meson in the  $D\bar{D}$  decay mode. The measured cross sections are presented in Figs.8a,b,c for  $D\bar{D}$ ,  $D^*\bar{D}$ , and  $D^*\bar{D}^*$  modes respectively. While known charmonium states are seen well, no sign of  $Y(4260)$  is observed; so only upper limits on  $Y(4260)$  branching fractions into  $D\bar{D}$  are set. It has been proved that  $BF(Y(4260) \rightarrow D\bar{D}) < BF(Y(4260) \rightarrow J/\psi\pi^+\pi^-)$ .

**Production of baryons** The first *BABAR* ISR baryon experiment was the measurement of the proton electromagnetic form factor (FF) [14] in the reaction  $e^+e^- \rightarrow p\bar{p}\gamma$ . The *BABAR* proton FF data, presented in Fig.9, in general agree with the previous measurements, confirm the rise of the proton FF at the threshold and modestly satisfy the QCD fit formula [15] above 2.5 GeV. Structures at 2.15 and 2.9 GeV are possibly seen. Study of the angular distribution allows to extract the value of  $|G_E/G_M|$  (the ratio of the electric and magnetic

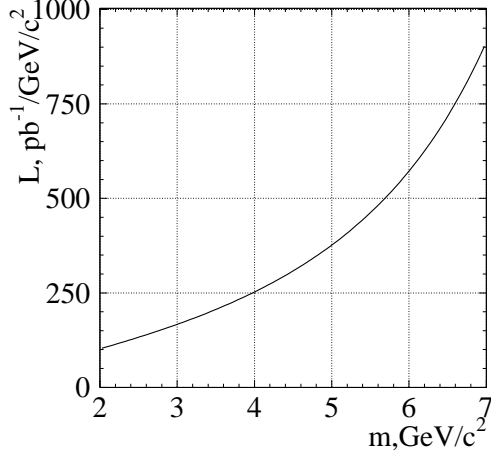


Figure 1: The mass dependence of ISR luminosity, calculated for the *BABAR* luminosity of 454 1/fb and the ISR photon angle range  $20^\circ < \theta_\gamma^* < 160^\circ$ .

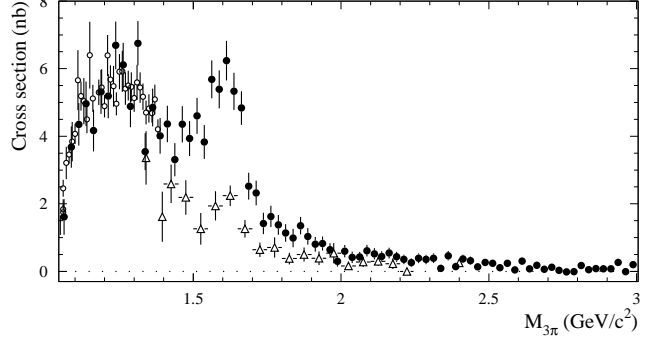


Figure 2: The  $e^+e^- \rightarrow \pi^+\pi^-\pi^0$  cross section, measured by SND (open circles), DM2 (open triangles), and *BABAR* (filled circles).

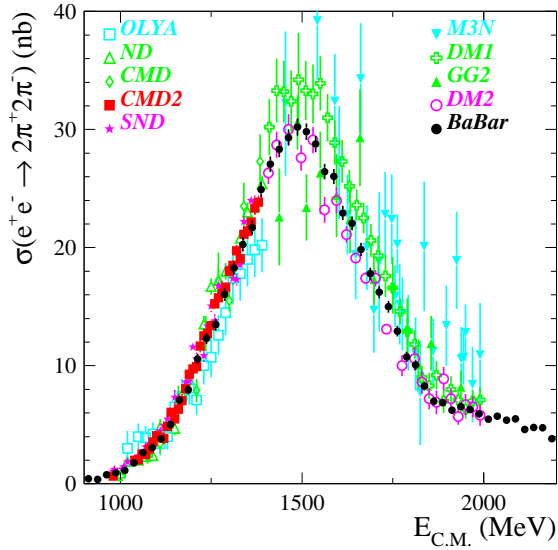


Figure 3: The comparison of the  $e^+e^- \rightarrow \pi^+\pi^-\pi^+\pi^-$  cross section, measured in *BABAR* experiment with the results of previous measurements.

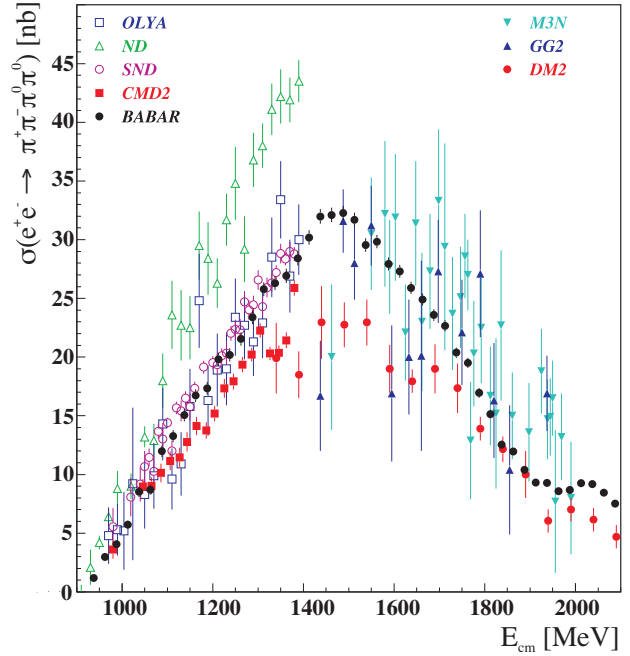


Figure 4: The comparison of the  $e^+e^- \rightarrow \pi^+\pi^-\pi^0\pi^0$  cross section, measured in *BABAR* experiment (preliminary data) with the results of previous measurements. An enhancement near 2.1 GeV is seen.

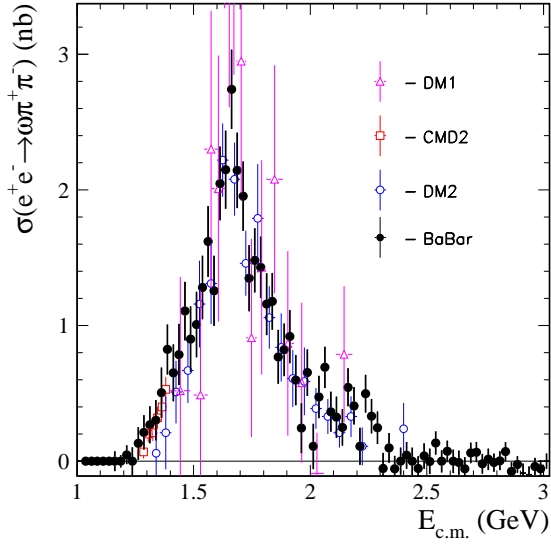


Figure 5: The comparison of the  $e^+e^- \rightarrow \omega\pi^+\pi^-$  cross section, measured in *BABAR* experiment with the results of previous measurements.

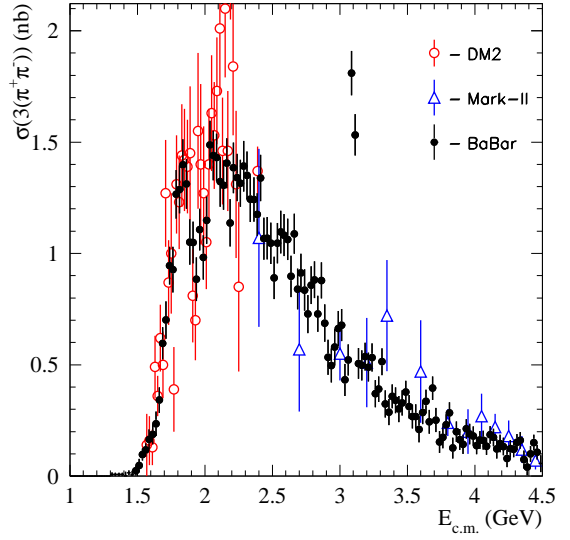


Figure 6: The comparison of the  $e^+e^- \rightarrow 3(\pi^+\pi^-)$  cross section, measured in *BABAR* experiment with the results of previous measurements. A dip near 1.9 GeV is seen.

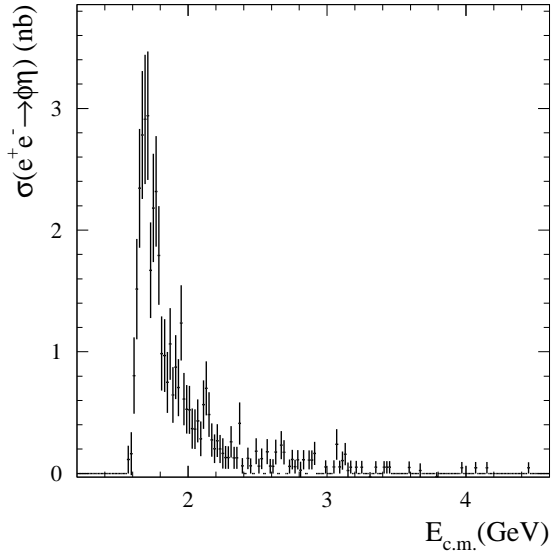


Figure 7: The  $e^+e^- \rightarrow \phi\eta$  cross section measured in *BABAR* experiment. An enhancement at 2.15 GeV is seen.

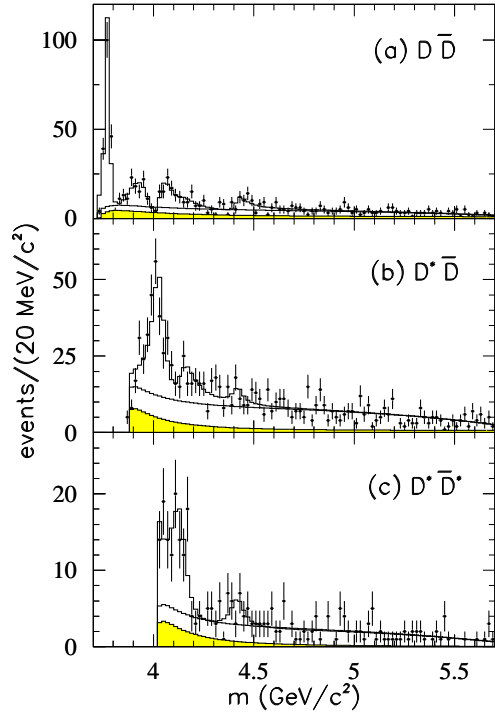


Figure 8: The *BABAR* ISR measurements of the  $e^+e^- \rightarrow D\bar{D}$ ,  $D^*\bar{D}$ , and  $D^*\bar{D}^*$  cross sections.

FFs) (Fig.10), which is found to be contradicting the only previous measurement at LEAR [16].

Later on the reactions  $e^+e^- \rightarrow \Lambda\bar{\Lambda}, \Sigma\bar{\Sigma}, \Lambda\bar{\Sigma}(\Sigma\bar{\Lambda})$  have been studied [17] and corresponding FFs are measured as well. The most accurate FF measurement is done for  $\Lambda$ . Previously the  $\Lambda$  FF was measured by DM2 only [18] in a single energy point. The *BABAR* data on the  $\Lambda$  and proton FF are shown in Fig.11. The asymptotic QCD prediction [19] for the ratio of the  $\Lambda$  and proton FF is 0.24. Figure 11 shows the strong disagreement between the data and prediction below 2.5 GeV. The disagreement at higher masses is less, but the measurements accuracy is not sufficient for the test of the prediction.

**Resonance physics** The number of produced events of narrow resonance with ISR is described by the expression  $N_{res} = \sigma_{res} \cdot L$ , where  $\sigma_{res} = \frac{12\pi^2\Gamma_{ee}B_f}{s m_{res}} \cdot W(s, x_0, \theta_0^*)$  is the ISR cross section and  $L$  is the total integrated luminosity. The  $x_0$  is related to the mass  $m_0$  of the resonance:  $x_0 = 1 - m_0^2/s$ . In the expression for the ISR cross section the  $\Gamma_{ee}$ ,  $B_f$  are the electron width and decay branching fraction, respectively. One can conclude from the above expression, that the number of events is determined by the electron width of the resonance.

Using the ISR technique, parameters of known vector states  $\rho(1450)$ ,  $\rho(1700)$ ,  $\omega(1420)$ ,  $\omega(1650)$  and  $\phi(1650)$  were improved (see above references on the cross section measurements). Concerning the  $J/\psi$  and  $\psi(2S)$  resonances, many decays were observed for the first time ( $J/\psi \rightarrow K^+K^-\pi^0\pi^0$ ,  $K^+K^-\pi^+\pi^-\eta$ ,  $K^{*0}K^{*0}$ ,  $\phi\pi^0 \dots$ ,  $\psi(2S) \rightarrow \pi^+\pi^-\pi^+\pi^-\eta$ ,  $K^+K^-\pi^+\pi^-\pi^+\pi^- \dots$ ), and the accuracies of many known decays were improved.

New vector states, found in ISR, deserve special attention. The most known is the charmonium-like  $Y(4260)$  resonance [20], decaying into  $J/\psi\pi^+\pi^-$ . It is relatively narrow (Fig.12),  $\Gamma = 92 \pm 15 \text{ MeV}/c^2$ , and has very low electron width  $\Gamma_{ee} = 7.5 \pm 1.1 \text{ eV}$ , which is much less than the value  $\sim 500 - 800 \text{ eV}$ , typical for  $\psi(4040)$ ,  $\psi(4160)$ ,  $\psi(4400)$  states. No decays of  $Y(4260)$  into  $D\bar{D}$  is seen. For these reasons the  $Y(4260)$  is considered as a candidate for the exotic 4-quark  $c\bar{c}n\bar{n}$  ( $n = u, d$ ) or molecular state. One could mention, that the  $\pi^+\pi^-$  mass spectrum in  $Y(4260)$  decay has a peak close to 1 GeV. This might be the indication of the contribution of  $J/\psi f_0(980)$  intermediate state.

Another new state is  $Y(4320)$  [21], decaying into  $\psi(2S)\pi^+\pi^-$ . Judging by presence of charmonium in the final state, narrow width and small production cross section this state might be of a similar nature as  $Y(4260)$ .

One more exotic candidate is the  $Y(2175)$  [22], first seen by *BABAR* in  $K^+K^-f_0(980)$ ,  $f_0 \rightarrow \pi^+\pi^-$ ,  $\pi^0\pi^0$  final states (Fig.13) and then in the  $\phi\eta$  (Fig.7) state. Similar to  $Y(4260)$  it is relatively narrow, has very low electron width and is considered as a possible  $s\bar{s}s\bar{s}$  exotic candidate or  $\phi''$  state.

Summarising the data on isovector channels one can suggest the existence of the new isovector state  $\rho(2150)$  or  $\rho'''$ . This resonance is seen in  $\pi^+\pi^-\pi^0\pi^0$  (Fig.4),  $\eta'(958)\rho^0$  [9] and  $p\bar{p}$  final states. In the latter case, we mean the step in the proton form factor near 2.15 GeV (Fig.9).

One should mention also about one more isovector candidate  $X(1880)$ , seen by *BABAR* as interference pattern (Fig.6) in the  $e^+e^- \rightarrow 6\pi$  cross section [10]. This state was seen earlier in DM2 [23] and FOCUS [24] experiments. The enhancement in the proton form factor at the threshold (Fig.9) can be due to this  $X(1880)$  state too.

**Conclusions** The  $e^+e^- \rightarrow \text{hadrons}$  cross sections are measured at *BABAR* in the energy

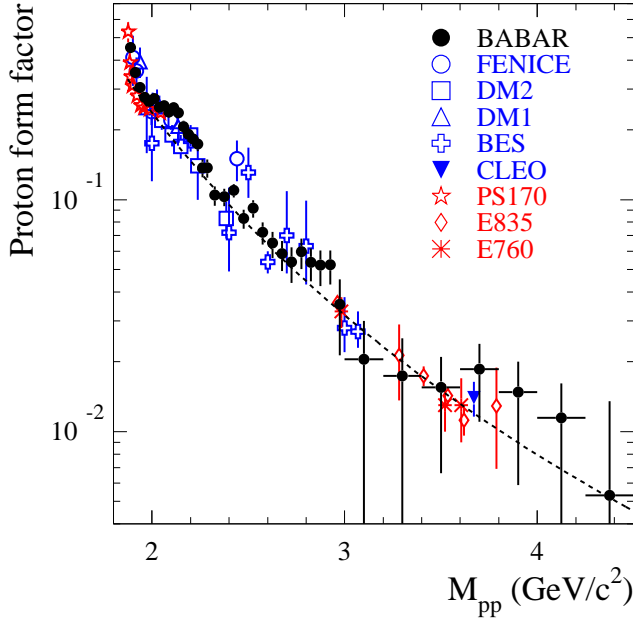


Figure 9: The proton form factor. The solid line corresponds to the QCD fit [15].

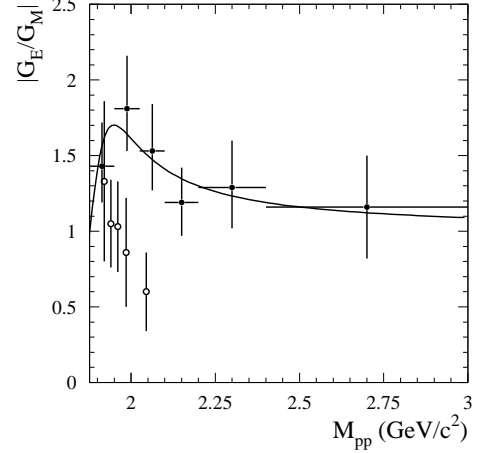


Figure 10: The measured by *BABAR*  $G_E/G_M$  ratio (black points), compared with LEAR data (open circles).

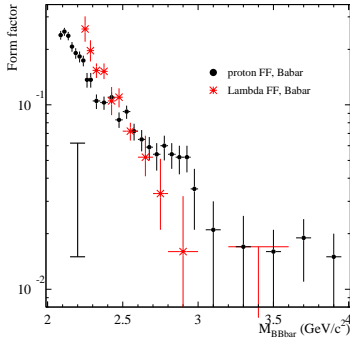


Figure 11: The comparison of proton and  $\Lambda$  form factors. Logarithmic scale. The vertical line corresponds to the asymptotic ratio between proton and  $\Lambda$  form factors.

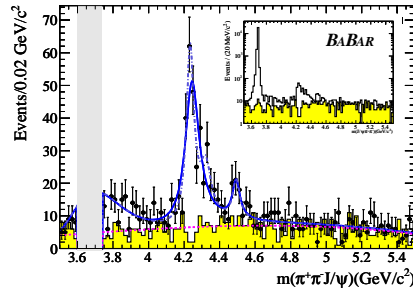


Figure 12: The  $J/\psi\pi^+\pi^-$  mass spectrum in the  $e^+e^- \rightarrow J/\psi\pi^+\pi^-\gamma$  reaction.

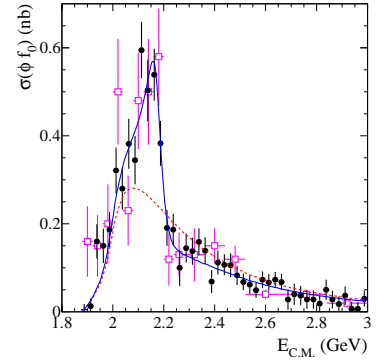


Figure 13: The *BABAR*  $e^+e^- \rightarrow \phi f_0$  cross section, measured in  $K^+K^-\pi^+\pi^-$  (filled circles) and  $K^+K^-\pi^0\pi^0$  (squares) final states.

range  $1 \div 5$  GeV using the ISR method. Parameters of many vector mesons ( $\rho, \omega, \phi$  excitations and the  $J/\psi$  and  $\psi(2S)$  states) are improved. New resonances are observed via ISR: Y(4260), Y(4320), and Y(2175), which are candidates for exotic states. Also seen are two new isovector candidates  $\rho(2150)$  and X(1880).

## References

- [1] M. Benayoun et al., Mod. Phys. Lett. **A14**, 2605 (1999).
- [2] G. Bonneau and F. Martin, Nucl. Phys. **B27**, 381 (1971).
- [3] BABAR Collaboration, B. Aubert *et al.*, Nucl. Instr. and Meth. A **479**, 1 (2002).
- [4] BABAR Collaboration, B. Aubert *et al.*, Phys. Rev. D **70**, 072004 (2004).
- [5] SND Collaboration, M. N. Achasov *et al.*, Phys. Rev. D **66**, 032001 (2002).
- [6] DM2 Collaboration, A. Antonelli *et al.*, Z. Phys. C **56**, 15 (1992)
- [7] BABAR Collaboration, B. Aubert *et al.*, Phys. Rev. D **71**, 052001 (2005).
- [8] V. P. Druzhinin, arxiv: hep-ex/0710.3455 (2007).
- [9] BABAR Collaboration, B. Aubert *et al.*, Phys. Rev. D **76**, 092005 (2007); erratum-ibid, **77**, 119902 (2008).
- [10] BABAR Collaboration, B. Aubert *et al.*, Phys. Rev. D **73**, 052003 (2006).
- [11] BABAR Collaboration, B. Aubert *et al.*, Phys. Rev. D **77**, 092002 (2008).
- [12] BABAR Collaboration, B. Aubert *et al.*, Phys. Rev. D **74**, 091103 (2006).
- [13] BABAR Collaboration, B. Aubert *et al.*, Phys. Rev. D **79**, 092001 (2009).
- [14] BABAR Collaboration, B. Aubert *et al.*, Phys. Rev. D **73**, 012005 (2006); hep-ex/05112023.
- [15] V. L. Chernyak, A. R. Zhitnitsky, JETP Lett. **25**, 510 (1977).
- [16] PS170 Collaboration, G. Bardin *et al.*, Nucl. Phys. **B411**, 3 (1994).
- [17] BABAR Collaboration, B. Aubert *et al.*, Phys. Rev. D **76**, 092006 (2007); hep-ex/0709.1988.
- [18] DM2 Collaboration, D. Bisello *et al.*, Z. Phys. C **48**, 23 (1990).
- [19] V. L. Chernyak *et al.*, Z. Phys. C **42**, 569 (1989).
- [20] BABAR Collaboration, B. Aubert *et al.*, Phys. Rev. Lett. **95**, 142001 (2005).
- [21] BABAR Collaboration, B. Aubert *et al.*, Phys. Rev. Lett. **98**, 912001 (2007).



- [22] *BABAR* Collaboration, B. Aubert *et al.*, Phys. Rev. D **74**, 091103 (2006).
- [23] A. B. Clegg, A. Donnachie, Z. Phys. C **45**, 677 (1990).
- [24] FOCUS Collaboration, P. L. Frabetti *et al.*, Phys. Lett. **B514**, 240 (2000).